Journal Pre-proofs

Green solvent-based extraction of Annona muricata L. (soursop) leaves: Influence on physicochemical properties, phytochemical content, and antioxidant activity

Hasdian Mudin, Mohammad Amil Zulhilmi Benjamin, Mohd Azrie Awang, Muhammad Naufal Qaweim Rushdy, Muhammad Daniel Eazzat Mohd Rosdan, Aniza Saini 1 and Dwi Setijawati

Please cite this article as: Hasdian Mudin, Mohammad Amil Zulhilmi Benjamin, Mohd Azrie Awang, Muhammad Naufal Qaweim Rushdy, Muhammad Daniel Eazzat Mohd Rosdan, Aniza Saini 1 and Dwi Setijawati, Green solvent-based extraction of Annona muricata L. (soursop) leaves: Influence on physicochemical properties, phytochemical content, and antioxidant activity, *Innovative Food Technologies (2025)*,
doi: https://doi.org/ 10.22104/ift.2025.8033.2257

Green solvent-based extraction of *Annona muricata* L. (soursop) leaves: Influence on physicochemical properties, phytochemical content, and antioxidant activity

Hasdian Mudin [1], Mohammad Amil Zulhilmi Benjamin [2], Mohd Azrie Awang [1,3]*, Muhammad Naufal Qaweim Rushdy [1], Muhammad Daniel Eazzat Mohd Rosdan [1], Aniza Saini [1] and Dwi Setijawati [4]

[1] Faculty of Food Science and Nutrition, Universiti Malaysia Sabah, Jalan UMS, Kota Kinabalu 88400, Sabah, Malaysia

[2] Borneo Research on Algesia, Inflammation and Neurodegeneration (BRAIN) Group, Faculty of Medicine and Health Sciences, Universiti Malaysia Sabah, Jalan UMS, Kota Kinabalu 88400, Sabah, Malaysia

[3] Food Security Research Laboratory, Faculty of Food Science and Nutrition, Universiti Malaysia Sabah, Jalan UMS, Kota Kinabalu 88400, Sabah, Malaysia

[4] Faculty of Fisheries and Marine Sciences, Universitas Brawijaya, Jl. Veteran, Ketawanggede, Lowokwaru, Malang 65145, Jawa Timur, Indonesia

*Corresponding author
Ts. Dr. Mohd Azrie Awang
Food Security Research Laboratory,
Faculty of Food Science and Nutrition,
Universiti Malaysia Sabah,
Jalan UMS, 88400 Kota Kinabalu, Sabah, Malaysia.
Email address: ma.awang@ums.edu.my

Running title: Green extraction of *Annona muricata* leaves

Abstract

Annona muricata L. (soursop) leaves are recognised as valuable sources of phenolic compounds with strong antioxidant potential, although conventional solvent extraction often provides limited selectivity and inadequate recovery of key bioactive constituents. Natural deep eutectic solvents (NADES) represent a greener extraction alternative, yet their performance in recovering phenolics, flavonoids, rutin, and antioxidant components from *A. muricata* leaf extract (AMLE) remains insufficiently explored. This study evaluated four NADES formulations, namely choline chloride–lactic acid (ChCl–LA), citric acid–L-proline (CA–LP), betaine–lactic acid (B–LA), and choline chloride–glycerol (ChCl–G), in comparison with water using ultrasound-assisted extraction. Physicochemical properties of the solvents, including pH and viscosity, were determined prior to extraction to elucidate their influence on solvent–solute interactions and extraction behaviour. Extraction efficiency was assessed through rutin content, total phenolic content (TPC), total flavonoid content (TFC), and antioxidant activities measured by DPPH, ABTS, and FRAP assays. All NADES systems exhibited acidic pH (1.80–4.97) and substantially higher viscosity than water, with ChCl–LA combining strong acidity and comparatively low viscosity, favourable for mass transfer. ChCl–LA demonstrated the strongest extraction of targeted bioactive constituents, achieving 164.16 ± 2.34 mg GAE/g TPC, 16.55 ± 0.52 mg QE/g TFC, 0.796 ± 0.023 mg/g rutin, and consistently high antioxidant activities across all assays. Correlation analysis indicated that FRAP activity was strongly associated with TPC, while DPPH and ABTS activities showed stronger associations with rutin and TFC, highlighting the contribution of different phenolic subclasses to antioxidant responses. The results demonstrate that solvent physicochemical properties, particularly acidity and viscosity, play a critical role in governing bioactive selectivity and antioxidant performance. ChCl–LA was identified as the

most effective green solvent for producing antioxidant-rich AMLE suitable for development of functional foods and nutraceutical products.

Keywords: *Annona muricata*; NADES; Ultrasound-assisted extraction; Rutin; Antioxidant

1. Introduction

Medicinal plants are widely recognised as important sources of natural products that contain phenolic acids, flavonoids, alkaloids, terpenoids, tannins, and other antioxidant metabolites with therapeutic relevance, contributing to the management of inflammation, oxidative stress, metabolic disorders, infections, and various chronic conditions [1]. Growing concern over the limitations of synthetic drugs, which may cause adverse effects, toxicity, high treatment costs, or reduced effectiveness arising from prolonged use or drug resistance, has intensified interest in safer and more sustainable plant-derived alternatives [2]. The extraction of these bioactive constituents requires appropriate solvent systems because solvent choice plays a central role in determining extraction efficiency, selectivity, and the overall phytochemical profile obtained from plant materials [3]. Conventional solvents such as water, methanol, ethanol, and acetone remain widely used for polar compound extraction, although water, despite its environmental benefits, often shows lower effectiveness in recovering certain phenolic and flavonoid compounds when compared with emerging green alternatives [4,5], highlighting the need for solvent systems that are both efficient and environmentally sustainable.

Natural deep eutectic solvents (NADES) have emerged as an important class of green solvents that provide sustainable alternatives to conventional organic systems due to their biodegradability, low toxicity, minimal volatility, and simple preparation requirements [6,7]. These solvents are typically produced by combining a hydrogen bond acceptor (HBA) such as choline chloride with hydrogen bond donors (HBD) that include lactic acid, glycerol, amino acids, or organic acids, forming structured liquid networks capable of extensive hydrogen-bonding with plant metabolites [8]. Numerous studies have demonstrated the superior extraction efficiency of NADES, as shown by enhanced phenolic recovery from black chokeberry fruits [9], high yields of bioactive compounds from *Lippia citriodora* using choline chloride–lactic acid (ChCl–LA) [10], and successful applications in mangosteen peel and *Mangifera pajang* extractions [11,12]. The performance of NADES is further strengthened when combined with ultrasound-assisted extraction (UAE), which applies acoustic cavitation to disrupt cell walls, increase solvent penetration, and accelerate mass transfer, thereby reducing extraction time and preserving heat-sensitive constituents [3,13]. Recent investigations confirm that the integration of NADES with UAE significantly improves phenolic and flavonoid extraction across various plant matrices [12,14], highlighting their complementary role as effective green extraction technologies.

Annona muricata L., commonly known as soursop and referred to as durian belanda in Malaysia, is a lowland tropical fruit tree from the Annonaceae family with a long record of traditional use in treating diabetes, hypertension, inflammation, infections, and cancer-related conditions. The leaves contain phenolic acids, flavonoids such as rutin, alkaloids, and acetogenins that contribute to a wide range of therapeutic activities, including antioxidant, anti-ulcer, anti-diabetic, antihypertensive, and wound-healing properties [15]. Scientific evidence shows that *A. muricata* leaf extract (AMLE) possesses strong antioxidant capacity that correlates with its phenolic and

flavonoid composition [16,17], emphasising the need for efficient extraction strategies to maximise the recovery of these compounds. Although the medicinal value of AMLE is well documented, its practical utilisation is restricted by limited optimisation of environmentally friendly extraction methods, and most studies continue to rely on conventional solvents or examine only a single deep eutectic solvent system [18,19]. Comparative evaluation of multiple NADES formulations for extracting phenolics, flavonoids, rutin, and antioxidant constituents from AMLE remains scarce, creating a gap in identifying solvent compositions that offer superior extraction efficiency and selectivity for different classes of bioactive metabolites.

This study addressed these limitations by evaluating four NADES systems, namely ChCl–LA, citric acid–L-proline (CA–LP), betaine–lactic acid (B–LA), and choline chloride–glycerol (ChCl–G), in comparison with water for UAE of AMLE. Extraction performance was examined through measurements of rutin content, total phenolic content (TPC), total flavonoid content (TFC), and antioxidant activity assessed using 2,2-diphenyl-1-picrylhydrazyl (DPPH), 2,2'-azino-bis(3-ethylbenzothiazoline-6-sulfonic acid) (ABTS), and ferric reducing antioxidant power (FRAP) assays. The outcomes offer essential guidance for identifying suitable green solvent systems that enhance the recovery of antioxidant-rich phytochemicals from AMLE for potential applications in functional foods and nutraceutical products.

2. Materials and methods

2.1. Plant materials

Fresh *A. muricata* leaves were collected from Tuaran, Sabah, Malaysia. The leaves were washed with distilled water and dried in an oven (ED 23, Binder, Tuttlingen, Germany) at 50 °C for 6 h. The dried samples were ground using a laboratory grinder to obtain a uniform powder and stored in resealable plastic bags at room temperature until analysis.

2.2. NADES preparation

Four NADES formulations were prepared as shown in Table 1, and the designated HBA and HBD for each system were weighed according to their specific molar ratios before being combined in glass beakers to form the initial mixtures. After eutectic formation, deionised water at 50% (w/w) was added to facilitate proper mixing, allowing the components to interact efficiently during the preparation process. The mixtures were then heated to 70 °C with continuous magnetic stirring at 500 rpm until clear and homogeneous liquids were obtained, after which they were allowed to cool to room temperature and were stored in sealed amber bottles until use.

Table 1
Composition of NADES formulations used for extracting *A. muricata* leaves.

2.3. Physicochemical determination

The physicochemical properties of water and NADES systems, including pH and viscosity, were determined prior to extraction. pH measurements were performed at room temperature using a calibrated digital pH meter (Mettler Toledo, Columbus, OH, USA) according to Darvishi et al. [24], with slight alterations. The pH meter was calibrated using standard buffer solutions at pH 4.0, 7.0, and 10.0, and measured values were corrected using calibration offsets to ensure accuracy. Viscosity measurements were conducted at room temperature following the method

described by Salehi and Vejdanivahid [25], with slight alterations, using a rotational viscometer (AMETEK Brookfield, Middleboro, MA, USA), and results were expressed in mPa·s.

2.4. Sample extraction

UAE was performed following Awang et al. [26] with minor modifications, and 5 g of dried *A. muricata* leaf powder were mixed with 100 mL of extraction solvent to achieve a 1:20 g/mL solid-to-solvent ratio before being subjected to five different solvent systems consisting of four NADES formulations and water as the control. Extraction was conducted using an ultrasonic probe sonicator (Q500 Sonicator, QSonica, Newtown, CT, USA) fitted with a 13 mm diameter probe, operating at 53% amplitude for 11 min and an 87% duty cycle at room temperature based on the conditions optimised by Saini et al. [20] with minor adjustments. Following extraction, the mixtures were filtered through Whatman No. 1 filter paper under vacuum and the resulting filtrates were stored at −20 °C until further analysis.

2.5. Rutin content

Rutin content was determined following Marinov et al. [27] using an Agilent 1100 high-performance liquid chromatography system with a diode array detector and an InertSustain C_{18} column (5 μm, 150 × 4.6 mm). The mobile phases were 0.1% formic acid in water (A) and 0.1% formic acid in acetonitrile (B), and the gradient was set at 10.0% B at 0 min, 20.0% B at 10 min, 95.0% B from 20 to 25 min, and 10.0% B from 25.10 to 30 min. The flow rate was maintained at 1.0 mL/min, the column temperature at 25 °C, the injection volume at 8.0 μL, and detection at 354 nm. The AMLE was filtered through a 0.22 μm PTFE membrane before injection, and rutin content was calculated from a calibration curve and expressed as mg/g of sample mass using Equation (1).

$$\text{Rutin content (mg/g)} = \frac{c \times V}{m} \tag{1}$$

where c represents the concentration of the sample extract (mg/L) obtained from the standard curve of rutin content, V represents the solvent volume (mL), and m represents the sample mass (g).

2.6. Total phenolic content

TPC was quantified using the Folin–Ciocalteu colorimetric method following Zulkifli et al. [28] with minor adjustments. A volume of 500 μL of AMLE was mixed with 500 μL of Folin–Ciocalteu reagent, followed by 1.5 mL of 20% sodium carbonate, and the mixture was topped up to 10 mL with deionised water. The reaction mixture was incubated in the dark for 2 h, after which absorbance was recorded at 765 nm using a UV–Vis spectrophotometer (Lambda 25, PerkinElmer, Waltham, MA, USA). TPC was calculated from a gallic acid calibration curve and expressed as mg GAE/g of sample mass using Equation (2).

$$\text{TPC (mg GAE/g)} = \frac{c \times V}{m} \tag{2}$$

where c represents the concentration of the sample extract (mg/L) obtained from the standard curve of TPC, V represents the solvent volume (mL), and m represents the sample mass (mg).

2.7. Total flavonoid content

TFC was quantified using the aluminium chloride colorimetric assay described by Rushdy et al. [29]. A volume of 1 mL of AMLE was mixed with 1 mL of 2% aluminium chloride, and the mixture was incubated in the dark for 15 min before absorbance was measured at 430 nm. TFC

was determined using a quercetin calibration curve and expressed as mg QE/g of sample mass using Equation (3).

$$\text{TFC (mg QE/g)} = \frac{c \times V}{m} \tag{3}$$

where c represents the concentration of the sample extract (mg/L) obtained from the standard curve of TFC, V represents the solvent volume (mL), and m represents the sample mass (mg).

2.8. DPPH radical scavenging assay

The DPPH assay was conducted following Mudin et al. [30] with minor modifications. A total of 1 mL of AMLE was mixed with 1 mL of 0.1 mM DPPH solution, and the mixture was incubated in the dark for 30 min before absorbance was measured at 517 nm using a microplate reader (Multiskan SkyHigh, Thermo Fisher Scientific, Waltham, MA, USA). Trolox served as the positive control, and DPPH inhibition (%) was calculated using Equation (4).

$$\text{DPPH inhibition (\%)} = \frac{\text{Abs}_{\text{control}} - \text{Abs}_{\text{sample}}}{\text{Abs}_{\text{control}}} \times 100 \tag{4}$$

where $\text{Abs}_{\text{control}}$ is the absorbance of the control (DPPH solution without sample mass) and $\text{Abs}_{\text{sample}}$ is the absorbance of the sample (DPPH solution with sample mass).

2.9. ABTS radical scavenging assay

The ABTS assay was conducted following Hussen and Endalew [31] with minor modifications. The ABTS radical was generated by reacting 1 mL of 7 mM ABTS with 1 mL of 2.45 mM potassium persulphate in a 1:1 ratio, and the mixture was incubated in the dark for 24 h before being diluted to an absorbance of 0.70 ± 0.02 at 734 nm. A total of 180 μL of AMLE was then mixed with 1.8 mL of ABTS reagent in a 2 mL microcentrifuge tube, followed by incubation for 5 min, and absorbance was measured at 734 nm. The ABTS reagent without extract served as the blank, Trolox was used as the positive control, and ABTS inhibition (%) was calculated using Equation (5).

$$\text{ABTS inhibition (\%)} = \frac{\text{Abs}_{\text{control}} - \text{Abs}_{\text{sample}}}{\text{Abs}_{\text{control}}} \times 100 \tag{5}$$

where $\text{Abs}_{\text{control}}$ is the absorbance of the control (ABTS solution without sample mass) and $\text{Abs}_{\text{sample}}$ is the absorbance of the sample (ABTS solution with sample mass).

2.10. FRAP assay

The FRAP assay was conducted following Russo et al. [32] with slight modifications. The FRAP reagent was prepared by combining 38 mM acetate buffer (pH 3.6), 10 mM TPTZ dissolved in 40 mM HCl, and 20 mM ferric chloride at a 10:1:1 ratio to ensure proper chromogenic complex formation. A total of 100 μL of AMLE was mixed with 900 μL of the freshly prepared FRAP reagent in a 2 mL microcentrifuge tube and incubated at 37 °C for 40 min to allow complete reduction of the ferric–TPTZ complex. Absorbance was subsequently measured at 593 nm, and FRAP values were quantified using a Trolox calibration curve, with the final results expressed as mg TE/g of sample mass according to Equation (6).

$$\text{FRAP (mg TE/g)} = \frac{c \times V}{m} \tag{6}$$

where c represents the concentration of the sample extract (mg/L) obtained from the standard curve of FRAP, V represents the solvent volume (mL), and m represents the sample mass (mg).

2.11. Statistical analysis

All experiments were conducted in triplicate and the results were expressed as mean ± standard deviation. Statistical analysis was performed using IBM SPSS Statistics (Version 28). One-way analysis of variance (ANOVA) was applied to determine significant differences between extraction solvents, and Tukey's HSD post-hoc test was used when significant effects were detected at $p < 0.05$. Pearson correlation analysis was conducted to assess relationships between the measured parameters, with statistical significance interpreted at $p < 0.01$.

3.   Results and discussion

3.1.   Green solvent effects on physicochemical properties of AMLE

The physicochemical properties of water and the prepared NADES systems, including corrected pH and viscosity, are summarised in Table 2. Water exhibited a near-neutral corrected pH of 7.51 ± 0.01 and the lowest viscosity at 0.89 ± 0.02 mPa·s, which were significantly different from all NADES systems ($p < 0.05$). All NADES formulations were acidic, with corrected pH values ranging from 1.80 ± 0.02 to 4.97 ± 0.05, and each solvent showed statistically significant differences from one another ($p < 0.05$). ChCl–LA exhibited the lowest pH (1.80 ± 0.02), followed by B–LA (2.52 ± 0.03) and CA–LP (2.72 ± 0.01), while ChCl–G showed the highest pH among the NADES systems (4.97 ± 0.05). In contrast to water, all NADES systems displayed substantially higher viscosities, ranging from 46.00 ± 0.01 to 221.00 ± 0.02 mPa·s, with statistically significant differences observed among all solvents ($p < 0.05$). ChCl–LA showed the lowest viscosity among the NADES formulations (46.00 ± 0.01 mPa·s), followed by B–LA (74.00 ± 0.01 mPa·s) and CA–LP (182.00 ± 0.02 mPa·s), while ChCl–G exhibited the highest viscosity (221.00 ± 0.02 mPa·s). These results demonstrate clear and statistically significant differences in both acidity and rheological behaviour across the solvent systems, which are expected to influence solvent–solute interactions and extraction performance.

Table 2
Corrected pH and viscosity values of water and NADES systems used for AMLE extraction.

The observed variations in pH and viscosity among NADES formulations reflect differences in hydrogen bond donor strength, molecular structure, and intermolecular interactions within each system. According to Sazali et al. [33] and Jablonský and Jančíková [34], the strongly acidic and relatively low-viscosity nature of ChCl–LA can be attributed to lactic acid, which provides high proton availability while maintaining a flexible hydrogen-bonding network, thereby enhancing solvent mobility and mass transfer. In contrast, the higher viscosity of ChCl–G is associated with extensive hydrogen-bonding interactions involving glycerol, which form dense solvent networks that restrict molecular diffusion despite its moderate acidity [33,35]. CA–LP exhibited intermediate acidity and high viscosity, reflecting the combined effects of citric acid and L-proline, which promote strong intermolecular interactions and reduced fluidity [35,36]. B–LA displayed moderate acidity and viscosity, suggesting a balance between proton availability and hydrogen-bond network density [33,37]. Collectively, these physicochemical properties play a crucial role in governing solvent–solute interactions, diffusion behaviour, and extraction performance, highlighting the importance of considering pH and viscosity together when evaluating NADES efficiency for phytochemical extraction.

3.2.   Green solvent effects on rutin content of AMLE

Figure 1 presents the rutin content obtained from AMLE using four NADES formulations and water. Rutin content measured by HPLC showed clear differences among green solvents. ChCl–LA recorded the highest rutin content at 0.796 ± 0.023 mg/g, which was statistically comparable with water at 0.780 ± 0.018 mg/g ($p > 0.05$). CA–LP and B–LA produced moderate rutin values of 0.509 ± 0.015 mg/g and 0.516 ± 0.015 mg/g, respectively ($p < 0.05$ versus ChCl–LA and water), while ChCl–G recorded the lowest rutin content at 0.411 ± 0.012 mg/g ($p < 0.05$).

Figure 1

Rutin content of AMLE obtained using different NADES formulations. Values represent means $\pm$ standard deviations (n = 3). Different letters indicate significant differences based on one-way ANOVA followed by Tukey's HSD at $p < 0.05$.

Rutin extraction followed a distinct trend because this highly hydrophilic flavonoid glycoside, characterised by multiple hydroxyl groups and a rutinose disaccharide moiety, requires specific solvent–solute hydrogen-bonding interactions for efficient recovery [38]. ChCl–LA extracted rutin effectively because lactic acid creates a mildly acidic environment that promotes the dissociation of weak non-covalent interactions between rutin and cell wall components while forming multiple hydrogen bonds with rutin hydroxyl groups, and the choline chloride component enhances solubility through electrostatic and dipole-mediated interactions with the aromatic regions of the rutin structure [39,40]. Water also recovered rutin efficiently due to its high polarity and structural compatibility with the glycosylated moiety [41]. The reduced rutin recovery observed in CA–LP, B–LA, and ChCl–G is attributable to higher viscosity, which reduces diffusivity and slows the release of rutin bound within macromolecular complexes, while glycerol-based NADES form dense hydrogen-bonding networks that hinder the mobility of bulky glycosides [42,43]. Compared with previous studies reporting higher rutin levels expressed per gram of extract in solvent-based extracts of *A. muricata* leaves, such as 11.52 ± 1.06 mg/g extract [17], the lower rutin values expressed per gram of plant material observed in the present study reflect differences in reporting basis, extraction strategy, solvent system, and analytical approach, as well as the limited number of available studies specifically quantifying rutin in this matrix. These findings indicate that rutin extractability is governed by solvent–solute compatibility and physicochemical properties rather than general extraction efficiency, and that solvent formulations must be tailored to match the structural and polarity characteristics of the target compound.

3.3.   Green solvent effects on phenolics and flavonoids of AMLE

Figure 2 presents the TPC and TFC obtained from AMLE using four NADES formulations and water, showing clear quantitative differences between solvents. TPC values varied significantly among all extraction systems ($p < 0.05$), with ChCl–LA recording the highest concentration at 164.16 ± 2.34 mg GAE/g, followed by CA–LP at 129.79 ± 1.52 mg GAE/g, ChCl–G at 90.64 ± 0.98 mg GAE/g, and B–LA at 82.81 ± 1.03 mg GAE/g, while water produced the lowest TPC at 15.24 ± 0.39 mg GAE/g. All NADES formulations generated significantly higher TPC values than water ($p < 0.05$). TFC measurements also demonstrated variability across solvents, with ChCl–LA yielding the highest TFC at 16.55 ± 0.52 mg QE/g, which was significantly higher than water at 9.65 ± 0.23 mg QE/g ($p < 0.05$). The remaining NADES formulations produced TFC values ranging from 9.11 ± 0.20 to 10.10 ± 0.22 mg QE/g, which did not differ significantly

from the TFC obtained with water ($p > 0.05$), as reflected in ChCl–G at 10.10 ± 0.22 mg QE/g, B–LA at 9.20 ± 0.25 mg QE/g, and CA–LP at 9.11 ± 0.20 mg QE/g.

Figure 2

TPC (bar) and TFC (line) of AMLE obtained using different NADES formulations. Values represent means $\pm$ standard deviations (n = 3). Different letters indicate significant differences based on one-way ANOVA followed by Tukey's HSD at $p < 0.05$.

Phenolic extraction is strongly governed by solvent polarity, hydrogen-bonding capacity, acidity, viscosity, and the ability to disrupt phenolic–polysaccharide associations within plant cell walls, and the superior TPC obtained with ChCl–LA and CA–LP reflects an optimal alignment of these characteristics. The mildly acidic environment created by lactic acid weakens ester linkages between phenolic acids and hemicellulose, facilitating the liberation of bound phenolics that typically remain inaccessible under neutral aqueous conditions [44]. The carboxyl and hydroxyl groups of lactic acid establish extensive hydrogen-bonding networks with phenolic hydroxyl groups, producing stable solvation shells that prevent molecular re-association and enhance solubility [39,40]. Choline chloride complements this behaviour by stabilising aromatic rings through Coulombic and dipole-driven interactions, enabling efficient solubilisation of hydroxybenzoic acids, hydroxycinnamic acids, and simple flavonoids [45]. CA–LP also achieved high TPC because citric acid contributes three carboxyl groups that form dense hydrogen-bonding matrices, while the cyclic structure of L-proline disrupts solvent ordering, reduces local microviscosity, and enhances penetration into compact tissue regions [46,47]. Lower TPC values obtained with B–LA and ChCl–G arise from weaker acidity and insufficient polarity gradients that do not efficiently cleave phenolic–cell wall ester linkages. Betaine, being zwitterionic, demonstrates preferential affinity for free phenolic acids but has limited ability to release esterified or glycosylated phenolics [48]. Glycerol-based NADES tend to solubilise a wider range of non-phenolic constituents, including carbohydrates, which dilutes the phenolic fraction [49]. Water produced the lowest TPC because phenolic–cell wall complexes require mild acidity or strong HBDs for effective cleavage, conditions not provided by water alone [50].

Flavonoid extraction displayed a distinct pattern because solvent composition influences flavonoid recovery differently from total phenolics. ChCl–LA produced the highest TFC due to its favourable interactions with the flavonoid chromone backbone and its ability to stabilise flavonoid glycosides under mildly acidic conditions. The lactic acid carboxyl group forms hydrogen bonds with hydroxyl moieties on the flavonoid rings, while its hydroxyl group associates with carbonyl centres, creating multipoint solvation that matches the polarity and structural requirements of flavonoids [51]. The remaining NADES formulations produced TFC values similar to water because the aluminium chloride assay responds broadly to ortho-dihydroxyl structures found not only in flavonoids but also in several non-flavonoid phenolics [52]. Flavonoids often remain bound to membrane proteins or accumulate in vacuoles, requiring stronger acidity or more specialised solute–solvent interactions for efficient extraction, conditions that were met primarily by ChCl–LA within this solvent system [51,53].

3.4. Green solvent effects on antioxidant activity of AMLE and their correlation with phytochemical content

Figure 3 presents the DPPH and ABTS radical scavenging activities and the FRAP reducing capacity of AMLE obtained using different solvents, showing significant differences across all assays ($p < 0.05$). ChCl–LA recorded the highest DPPH inhibition at 89.91 ± 0.66%, followed by B–LA at 88.83 ± 0.85% ($p < 0.05$ versus CA–LP and ChCl–G), with water yielding 86.53 ± 0.71% ($p < 0.05$ versus ChCl–G) and CA–LP and ChCl–G producing lower values at 78.73 ± 0.64% and 78.74 ± 0.97%, respectively. ABTS activity also differed significantly among solvents ($p < 0.05$), with ChCl–LA achieving the highest inhibition at 75.64 ± 1.42%, followed by B–LA at 64.34 ± 0.66%, water at 56.95 ± 0.99%, CA–LP at 52.45 ± 0.80%, and ChCl–G at 49.44 ± 0.64%, with all pairwise differences significant ($p < 0.05$). FRAP results showed significant variation among solvents ($p < 0.05$), with ChCl–LA producing the highest reducing capacity at 1252.12 ± 16.54 mg TE/g, followed by CA–LP at 1094.73 ± 13.67 mg TE/g, B–LA at 1022.55 ± 12.50 mg TE/g, and ChCl–G at 845.97 ± 14.00 mg TE/g. The FRAP value obtained using water (808.42 ± 14.02 mg TE/g) was statistically comparable with ChCl–G ($p > 0.05$).

Figure 3
DPPH (bar), ABTS (bar), and FRAP (line) of AMLE obtained using different NADES formulations. Values represent means ± standard deviations (n = 3). Different letters indicate significant differences based on one-way ANOVA followed by Tukey's HSD at $p < 0.05$.

Correlation analysis showed that rutin exhibited significant positive associations with DPPH (r = 0.712, $p < 0.01$) and ABTS (r = 0.663, $p < 0.01$) as presented in Table 3, whereas its correlation with FRAP was weak and non-significant (r = 0.273, $p > 0.05$). TPC demonstrated a weak non-significant correlation with DPPH (r = −0.026, $p > 0.05$) and a moderate non-significant correlation with ABTS (r = 0.450, $p > 0.05$), while showing a strong significant correlation with FRAP (r = 0.889, $p < 0.01$). TFC displayed a moderate correlation with DPPH (r = 0.506, $p > 0.05$) and strong significant correlations with ABTS (r = 0.799, $p < 0.01$) and FRAP (r = 0.677, $p < 0.01$). These findings indicate that the antioxidant assays responded to different phytochemical groups, with DPPH closely associated with rutin, ABTS strongly influenced by rutin and TFC, and FRAP primarily associated with TPC and TFC.

Table 3
Pearson correlation coefficients between phytochemical content (rutin, TPC, and TFC) and antioxidant activities (DPPH, ABTS, and FRAP) of AMLE.

The antioxidant behaviour of AMLE extracts reflects the combined influence of NADES-dependent variation in phenolic composition, the structural diversity of phenolic subclasses, and the mechanistic requirements of each antioxidant assay. The superior performance of ChCl–LA can be attributed to its chemical structure, where the choline chloride component provides strong hydrogen-bond acceptor capacity while lactic acid contributes multiple hydrogen-bond donor sites and mild acidity, collectively enhancing solubilisation of polyhydroxylated phenolics and flavonoid glycosides. ChCl–LA consistently produced the highest DPPH, ABTS, and FRAP activities because its mildly acidic matrix enhanced the solubilisation of phenolic compounds with strong hydrogen atom transfer and electron-donating capacity, including catechol-type structures, gallic acid derivatives, and polyhydroxylated flavonoids. The acidic environment

further promotes dissociation of phenolics bound to cell wall components, increasing extractable phenolic availability. These compounds stabilise free radicals through resonance delocalisation and multiple hydroxyl substitutions that facilitate efficient electron release [44,51].

The strong DPPH and ABTS activities observed in extracts containing higher rutin concentrations further reflect the high reactivity of rutin toward both hydrogen atom transfer and electron transfer pathways [54], consistent with its correlations with DPPH ($r = 0.712$) and ABTS ($r = 0.663$). In contrast, B–LA demonstrated strong DPPH activity despite lower TPC because its hydrogen-bonding network favours selective enrichment of phenolic subclasses with inherently high radical-scavenging potency rather than bulk phenolic extraction. CA–LP and ChCl–G exhibited lower antioxidant responses due to their higher viscosity and denser hydrogen-bonding networks, which restrict diffusivity and limit the release of highly reactive phenolics, particularly bulky glycosylated flavonoids. In addition, these solvents preferentially extracted phenolic acids and glycosylated flavonoids with weaker radical-scavenging reactivity, further contributing to reduced antioxidant responses under more viscous solvent conditions [47,55].

FRAP activity demonstrated the strongest dependence on total phenolic concentration, supported by the strong correlation between TPC and FRAP ($r = 0.889$), indicating preferential extraction of electron-donating phenolics such as flavonols, hydroxybenzoic acids, and hydroxycinnamic acids. This behaviour reflects the strong sensitivity of FRAP to phenolics capable of single-electron transfer, which are preferentially stabilised in NADES systems with balanced polarity and hydrogen-bonding capacity. TFC showed positive associations with both FRAP ($r = 0.677$) and ABTS ($r = 0.799$), suggesting that flavonoid subclasses contributed more strongly to electron-transfer mechanisms than to hydrogen atom transfer, while the moderate correlation between TFC and DPPH ($r = 0.506$) reflects the heterogeneous reactivity of flavonoids across different pathways. These relationships demonstrate that antioxidant capacity is influenced not only by total phenolic mass but also by the specific phenolic subclasses present in each extract, as indicated by the weaker associations between TPC and DPPH or ABTS relative to the strong TPC–FRAP relationship.

Overall, the observed trends highlight that solvent structure, acidity, and viscosity collectively govern solubilisation behaviour and mass transfer efficiency, thereby dictating the selective recovery of antioxidant-active phytochemical classes. The integration of UAE further strengthened solvent–phytochemical interactions by generating cavitation forces that disrupted cellular structures, enhanced solvent penetration, released cell wall-bound phenolics, and accelerated mass transfer [3,13]. The synergistic action between NADES chemistry and ultrasonic cavitation produced extracts enriched in structurally diverse phenolic compounds, thereby supporting broad-spectrum antioxidant activity across multiple mechanistic pathways [6,7].

3.5.   Future studies

Future studies should incorporate representative liquid chromatography (LC) chromatograms to provide visual and qualitative insights into the phytochemical profiles of AMLE extracts obtained using different green solvents, with particular emphasis on ChCl–LA as the most effective NADES identified in this study. Inclusion of chromatographic fingerprints, together

with peak annotation and LC–MS-assisted identification, would enable more detailed characterisation of individual compounds and comparison of solvent selectivity. In addition, further investigations should evaluate the Kamlet–Taft solvatochromic parameters of the NADES systems, especially ChCl–LA, to better elucidate solvent–solute interactions, mass transfer behaviour, and their influence on extraction efficiency. Such analyses would strengthen compound-level interpretation, support extract standardisation and quality control, and enable assessment of scalability, solvent recyclability, and economic feasibility, thereby facilitating future scale-up and industrial application of AMLE.

4.   Conclusions

This study demonstrated that NADES are effective green alternatives to water for extracting bioactive constituents from AMLE. Among the evaluated solvents, ChCl–LA was identified as the most efficient system due to its favourable physicochemical properties, characterised by strong acidity and comparatively low viscosity, which enhanced solvent–solute interactions and mass transfer during UAE. ChCl–LA achieved a 10.8-fold increase in TPC at 164.16 mg GAE/g and produced the highest antioxidant activities across DPPH, ABTS, and FRAP assays. These findings indicate that solvent selectivity and antioxidant performance are governed primarily by physicochemical characteristics of the solvent system rather than extract quantity alone. The integration of NADES with UAE provided a synergistic advantage through enhanced cell disruption, solvent penetration, and accelerated release of phenolic compounds. The overall findings confirm that AMLE are valuable sources of antioxidant-rich phytochemicals with potential for incorporation into functional foods and nutraceutical products. Future research should focus on detailed compound-level characterisation and optimisation of NADES formulations with consideration of physicochemical behaviour, scalability, and industrial applicability.

Conflict of interest

No conflict of interest has been declared by the authors.

Acknowledgments

References

[1]   Sun, W., & Shahrajabian, M. H. (2023). Therapeutic potential of phenolic compounds in medicinal plants—Natural health products for human health. *Molecules*, *28*(4), 1845. https://doi.org/10.3390/molecules28041845

[2]   El-Saadony, M. T., Saad, A. M., Mohammed, D. M., Korma, S. A., Alshahrani, M. Y., Ahmed, A. E., Ibrahim, E. H., Salem, H. M., Alkafaas, S. S., Saif, A. M., Elkafas, S. S., Fahmy, M. A., Abd El-Mageed, T. A., Abady, M. M., Assal, H. Y., El-Tarabily, M. K., Mathew, B. T., AbuQamar, S. F., El-Tarabily, K. A., & Ibrahim, S. A. (2025). Medicinal plants: bioactive compounds, biological activities, combating multidrug-resistant microorganisms, and human health benefits - A comprehensive review. *Frontiers in Immunology*, *16*, 1491777. https://doi.org/10.3389/fimmu.2025.1491777

[3]   Awang, M. A., Nik Mat Daud, N. N. N., Mohd Ismail, N. I., Abdullah, F. I., & Benjamin, M. A. Z. (2023). A review of *Dendrophthoe pentandra* (mistletoe): Phytomorphology,

extraction techniques, phytochemicals, and biological activities. *Processes*, *11*(8), 2348. https://doi.org/10.3390/pr11082348

[4] Anuar, A., Awang, M. A., & Tan, H. F. (2021). Impact of solvent selection on the extraction of total phenolic content and total flavonoid content from kaffir lime leaves: Ultrasonic assisted extraction (UAE) and microwave assisted extraction (MAE). *AIP Conference Proceedings*, *2347*, 020020. https://doi.org/10.1063/5.0051934

[5] Alqahtani, N. K., Mohamed, H. A., Moawad, M. E., Younis, N. S., & Mohamed, M. E. (2023). The hepatoprotective effect of two date palm fruit cultivars' extracts: Green optimization of the extraction process. *Foods*, *12*(6), 1229. https://doi.org/10.3390/foods12061229

[6] Chemat, F., Vian, M. A., Ravi, H. K., Khadhraoui, B., Hilali, S., Perino, S., & Tixier, A.-S. F. (2019). Review of alternative solvents for green extraction of food and natural products: Panorama, principles, applications and prospects. *Molecules*, *24*(16), 3007. https://doi.org/10.3390/molecules24163007

[7] Li, D. (2022). Natural deep eutectic solvents in phytonutrient extraction and other applications. *Frontiers in Plant Science*, *13*, 1004332. https://doi.org/10.3389/fpls.2022.1004332

[8] Prabhune, A., & Dey, R. (2023). Green and sustainable solvents of the future: Deep eutectic solvents. *Journal of Molecular Liquids*, *379*, 121676. https://doi.org/10.1016/j.molliq.2023.121676

[9] Razboršek, M. I., Ivanović, M., Krajnc, P., & Kolar, M. (2020). Choline chloride based natural deep eutectic solvents as extraction media for extracting phenolic compounds from chokeberry (*Aronia melanocarpa*). *Molecules*, *25*(7), 1619. https://doi.org/10.3390/molecules25071619

[10] Ivanović, M., Alañón, M. E., Arráez-Román, D., & Segura-Carretero, A. (2018). Enhanced and green extraction of bioactive compounds from *Lippia citriodora* by tailor-made natural deep eutectic solvents. *Food Research International*, *111*, 67–76. https://doi.org/10.1016/j.foodres.2018.05.014

[11] Plaza, M., Domínguez-Rodríguez, G., Sahelices, C., & Marina, M. L. (2021). A sustainable approach for extracting non-extractable phenolic compounds from mangosteen peel using ultrasound-assisted extraction and natural deep eutectic solvents. *Applied Sciences*, *11*(12), 5652. https://doi.org/10.3390/app11125625

[12] Mohd Rosdan, M. D. E., Awang, M. A., Benjamin, M. A. Z., Andrew, F. A., Saini, A., Mohd Amin, S. F., & Julmohammad, N. (2025). Natural deep eutectic solvents vs. conventional solvents: Effects on crude yield, mangiferin content, antioxidant activity, and toxicity in *Mangifera pajang* Kosterm. fruit extracts. *Malaysian Applied Biology*, *54*(1), 87–97. https://doi.org/10.55230/mabjournal.v54i1.3212

[13] Kumar, A., Nirmal, P., Kumar, M., Jose, A., Tomer, V., Oz, E., Proestos, C., Zeng, M., Elobeid, T., Sneha, K., & Oz, F. (2023). Major phytochemicals: Recent advances in health benefits and extraction method. *Molecules*, *28*(2), 887. https://doi.org/10.3390/molecules28020887

[14] Djaoudene, O., Bachir-Bey, M., Schisano, C., Djebari, S., Tenore, G. C., & Romano, A. (2024). A sustainable extraction approach of phytochemicals from date (*Phoenix dactylifera* L.) fruit cultivars using ultrasound-assisted deep eutectic solvent: A comprehensive study on bioactivity and phenolic variability. *Antioxidants*, *13*(2), 181. https://doi.org/10.3390/antiox13020181

[15] Zubaidi, S. N., Nani, H. M., Kamal, M. S. A., Qayyum, T. A., Maarof, S., Afzan, A., Misnan, N. M., Hamezah, H. S., Baharum, S. N., & Mediani, A. (2023). *Annona muricata*: Comprehensive review on the ethnomedicinal, phytochemistry, and pharmacological aspects focusing on antidiabetic properties. *Life*, *13*(2), 353. https://doi.org/10.3390/life13020353

[16] Nam, J.-S., Park, S.-Y., Jang, H.-L., & Rhee, Y. H. (2017). Phenolic compounds in different parts of young *Annona muricata* cultivated in Korea and their antioxidant activity. *Applied Biological Chemistry*, *60*(5), 535–543. https://doi.org/10.1007/s13765-017-0309-5

[17] Hartati, R., Rompis, F. M., Pramastya, H., & Fidrianny, I. (2024). Optimization of antioxidant activity of soursop (*Annona muricata* L.) leaf extract using response surface methodology. *Biomedical Reports*, *21*(5), 166. https://doi.org/10.3892/br.2024.1854

[18] Leal, F. C., Farias, F. O., do Amaral, W., Toci, A. T., Mafra, M. R., & Igarashi-Mafra, L. (2022). Green solvents to value *Annona muricata* L. leaves as antioxidants source: Process optimization and potential as a natural food additive. *Waste and Biomass Valorization*, *13*(2), 1233–1241. https://doi.org/10.1007/s12649-021-01581-0

[19] Oton, L. F., Ribeiro, P. R. V., de Brito, E. S., & de Santiago-Aguiar, R. S. (2025). Sustainable extraction of bioactive compounds from *Annona muricata* L. leaves by deep eutectic solvents (DESs). *ACS Omega*, *10*(16), 16909–16920. https://doi.org/10.1021/acsomega.5c01232

[20] Saini, A., Benjamin, M. A. Z., Mohd Rosdan, M. D. E., Mohamad Rosdi, M. N., & Awang, M. A. (2025). Response surface methodology-based optimised ultrasound-assisted extraction of phenolics from *Solanum lasiocarpum* Dunal (terung asam) fruit: Anti-diabetic evaluation and ADMET study. *Biocatalysis and Agricultural Biotechnology*, *68*, 103704. https://doi.org/10.1016/j.bcab.2025.103704

[21] Wu, H., Zhang, G., Zhang, Y., Guo, P., Wu, H., Gao, R., & Liu, T. (2025). Natural deep eutectic solvent (NADES)-aided extraction of bioactive compounds from cotton byproducts for agricultural applications: Extraction optimization, structural identification, and bioactivity evaluation. *Industrial Crops and Products*, *233*, 121389. https://doi.org/10.1016/j.indcrop.2025.121389

[22] Gutiérrez, A., Alcalde, R., Atilhan, M., & Aparicio, S. (2020). Insights on betaine + lactic acid deep eutectic solvent. *Industrial & Engineering Chemistry Research*, *59*(25), 11880–11892. https://doi.org/10.1021/acs.iecr.0c00762

[23] Motta, D., Mondahchouo, S., Nejrotti, S., Pontremoli, C., Barolo, C., Damin, A., & Bonomo, M. (2025). Glycerol-based deep eutectic solvents for efficient andreversible iodine uptakefrom vapour phase. *Communications Chemistry*, *8*(1), 178. https://doi.org/10.1038/s42004-025-01575-2

[24] Darvishi, H., Mohammadi, M., Behroozi-Khazaei, N., Jahani-Azizabadi, H., & Solaimani, M. (2025). Comparative analysis of ohmic heating and conventional evaporation for milk concentration: Quality parameters, energy and exergy efficiencies, GHG emission, and sensory evaluation. *Innovative Food Technologies*, *12*(3), 305–319. https://doi.org/10.22104/ift.2025.7710.2222

[25] Salehi, F., & Vejdanivahid, S. (2025). Effect of basil seed gum concentration on the physical, textural and sensory properties of quinoa pancakes. *Innovative Food Technologies*, *13*(1), 13–22. https://doi.org/10.22104/ift.2025.7821.2231

[26] Awang, M. A., Chua, L. S., Abdullah, L. C., & Pin, K. Y. (2021). Drying kinetics and optimization of quercetrin extraction from *Melastoma malabathricum* leaves. *Chemical Engineering and Technology*, *44*(7), 1214–1220. https://doi.org/10.1002/ceat.202100007

[27] Marinov, T., Kokanova-Nedialkova, Z., & Nedialkov, P. (2024). UHPLC-HRMS-based profiling and simultaneous quantification of the hydrophilic phenolic compounds from the aerial parts of *Hypericum aucheri* Jaub. & Spach (Hypericaceae). *Pharmacia*, *71*, 1–11. https://doi.org/10.3897/pharmacia.71.e122436

[28] Zulkifli, M. Z. A., Benjamin, M. A. Z., Mohd Rosdan, M. D. E., Saini, A., Rusdi, N. A., & Awang, M. A. (2025). Optimisation of yield, flavonoids, and antioxidant activity via ultrasound-assisted extraction of bamboo leaves from *Dinochloa sublaevigata* S. Dransf. (wadan) in Sabah, Malaysia. *Advances in Bamboo Science*, *10*, 100128. https://doi.org/10.1016/j.bamboo.2025.100128

[29] Rushdy, M. N. Q., Awang, M. A., Benjamin, M. A. Z., Mohd Rosdan, M. D. E., & Saini, A. (2025). Microwave drying of *Gnetum gnemon* L. leaves for functional foods and nutraceuticals: Kinetic modelling, colour attributes, phytochemical content, and antioxidant activity. *Food and Humanity*, *5*, 100868. https://doi.org/10.1016/j.foohum.2025.100868

[30] Mudin, H., Benjamin, M. A. Z., Rusdi, N. A., & Awang, M. A. (2025). Optimisation of fruit vinegar process from *Baccaurea lanceolata* (Miq.) Müll.Arg using central composite design with antioxidant and antimicrobial potential. *Jurnal Teknologi*, *87*(5), 987–998. https://doi.org/10.11113/jurnalteknologi.v87.23406

[31] Hussen, E. M., & Endalew, S. A. (2023). *In vitro* antioxidant and free-radical scavenging activities of polar leaf extracts of *Vernonia amygdalina*. *BMC Complementary Medicine and Therapies*, *23*(1), 146. https://doi.org/10.1186/s12906-023-03923-y

[32] Russo, D., Kenny, O., Smyth, T. J., Milella, L., Hossain, M. B., Diop, M. S., Rai, D. K., & Brunton, N. P. (2013). Profiling of phytochemicals in tissues from *Sclerocarya birrea* by HPLC-MS and their link with antioxidant activity. *ISRN Chromatography*, *2013*, 283462. https://doi.org/10.1155/2013/283462

[33] Sazali, A. L., AlMasoud, N., Amran, S. K., Alomar, T. S., Pa'ee, K. F., El-Bahy, Z. M., Yong, T.-L. K., Dailin, D. J., & Chuah, L. F. (2023). Physicochemical and thermal characteristics of choline chloride-based deep eutectic solvents. *Chemosphere*, *338*, 139485. https://doi.org/10.1016/j.chemosphere.2023.139485

[34] Jablonský, M., & Jančíková, V. (2023). Comparison of the acidity of systems based on choline chloride and lactic acid. *Journal of Molecular Liquids*, *380*, 121731. https://doi.org/10.1016/j.molliq.2023.121731

[35] Md Yusoff, M. H., Gan, C.-Y., & Shafie, M. H. (2023). Characterization of citric acid monohydrate-glycerol based deep eutectic solvents which could be used as an extraction medium for hydrophilic bioactive components. *Journal of Molecular Liquids*, *389*, 122879. https://doi.org/10.1016/j.molliq.2023.122879

[36] Sánchez, P. B., González, B., Salgado, J., Parajó, J. J., & Domínguez, Á. (2019). Physical properties of seven deep eutectic solvents based on L-proline or betaine. *The Journal of Chemical Thermodynamics*, *131*, 517–523. https://doi.org/10.1016/j.jct.2018.12.017

[37] Vorobyova, V., Skiba, M., Vinnichuk, K., Linyucheva, O., & Vasyliev, G. (2025). Influence of hydrogen bond donor compound type on the properties of betaine based deep eutectic solvents: A computational and experimental approach. *Journal of Molecular Structure*, *1323*, 140743. https://doi.org/10.1016/j.molstruc.2024.140743

[38] Tobar-Delgado, E., Mejía-España, D., Osorio-Mora, O., & Serna-Cock, L. (2023). Rutin: Family farming products' extraction sources, industrial applications and current trends in biological activity protection. *Molecules*, *28*(15), 5864. https://doi.org/10.3390/molecules28155864

[39] Wei, J., Ge, H., Zhu, B., Xu, Y., Wang, S., Li, B., & Xu, H. (2024). Probing the interaction mechanism of choline chloride-based deep eutectic solvents with flavonoid and polyphenol systems. *Journal of Molecular Liquids*, *408*, 125310. https://doi.org/10.1016/j.molliq.2024.125310

[40] Duan, Y., Meng, F., Manickam, S., Zhu, X., Yang, J., Han, Y., & Tao, Y. (2025). Four distinct pathways involved in a "tug-of-war" lead to the non-linear nature of phenolic chemistry during lactic acid fermentation of fruits and vegetables. *Journal of Advanced Research*. https://doi.org/10.1016/j.jare.2025.02.033

[41] Choi, S.-S., Park, H.-R., & Lee, K.-A. (2021). A comparative study of rutin and rutin glycoside: Antioxidant activity, anti-inflammatory effect, effect on platelet aggregation and blood coagulation. *Antioxidants*, *10*(11), 1696. https://doi.org/10.3390/antiox10111696

[42] Liu, C., Sun, W., & Liu, Q. (2022). Opinions on glycerol-based deep eutectic solvent nanofluids for energy transportation. *Frontiers in Energy Research*, *10*, 979857. https://doi.org/10.3389/fenrg.2022.979857

[43] Sani, N. F. A., Ramadhan, R., Yahaya, N., Ghadzi, S. M. S., Mohamed, A. H., Kamaruzaman, S., Ibrahim, W. N. W., Hanapi, N. S. M., & Zain, N. N. M. (2025). Advancements in deep eutectic solvent-based membranes for the extraction, separation, and preconcentration of organic compounds. *Advances in Sample Preparation*, *14*, 100181. https://doi.org/10.1016/j.sampre.2025.100181

[44] Zhang, L., Li, A., Liu, H., Mo, Q., & Zhong, Z. (2025). Effects of lactic acid bacteria fermentation on the release and biotransformation of bound phenolics in Ma bamboo shoots (*Dendrocalamus latiflorus* Munro). *Foods*, *14*(15), 2573. https://doi.org/10.3390/foods14152573

[45] Poe, D., Abranches, D. O., Wang, X., Klein, J., Dean, W., Hansen, B. B., Doherty, B., Fraenza, C., Gurkan, B., Sangoro, J. R., Tuckerman, M., Greenbaum, S. G., & Maginn, E. J. (2025). Structural and dynamic heterogeneity of deep eutectic solvents composed of choline chloride and ortho-phenol derivatives. *The Journal of Physical Chemistry B*, *129*(4), 1360–1375. https://doi.org/10.1021/acs.jpcb.4c06787

[46] Daniecki, N. J., Bhatt, M. R., Yap, G. P. A., & Zondlo, N. J. (2022). Proline C−H bonds as loci for proline assembly via C−H/O interactions. *ChemBioChem*, *23*(24), e202200409. https://doi.org/10.1002/cbic.202200409

[47] Książek, E. (2024). Citric acid: Properties, microbial production, and applications in industries. *Molecules*, *29*(1), 22. https://doi.org/10.3390/molecules29010022

[48] Wysocki, M., Stachowiak, W., Smolibowski, M., Olejniczak, A., Niemczak, M., & Shamshina, J. L. (2024). Rethinking the esterquats: Synthesis, stability, ecotoxicity and applications of esterquats incorporating analogs of betaine or choline as the cation in their structure. *International Journal of Molecular Sciences*, *25*(11), 5761. https://doi.org/10.3390/ijms25115761

[49] Chevé-Kools, E., Choi, Y. H., Roullier, C., Ruprich-Robert, G., Grougnet, R., Chapeland-Leclerc, F., & Hollman, F. (2025). Natural deep eutectic solvents (NaDES): Green solvents for pharmaceutical applications and beyond†. *Green Chemistry*, *27*, 8360. https://doi.org/10.1039/d4gc06386d

[50] Mandal, M. K., Gan, W., & Domb, A. J. (2025). Phenolate-based bioactive compounds: Design, delivery and biomedical applications. *Coordination Chemistry Reviews*, *544*, 216941. https://doi.org/10.1016/j.ccr.2025.216941

[51] Popović, B. M., Uka, D., Boublia, A., Agić, D., Kukrić, T., Albrahim, M., Elboughdiri, N., & Benguerba, Y. (2024). Solubility and extractability enhancement of the main food flavonoids by using choline chloride-based natural deep eutectic solvents. *Journal of Molecular Liquids*, *415*, 126333. https://doi.org/10.1016/j.molliq.2024.126333

[52] Kukhtenko, H., Bevz, N., Konechnyi, Y., Kukhtenko, O., & Jasicka-Misiak, I. (2024). Spectrophotometric and chromatographic assessment of total polyphenol and flavonoid content in *Rhododendron tomentosum* extracts and their antioxidant and antimicrobial activity. *Molecule*, *29*(5), 1095. https://doi.org/10.3390/molecules29051095

[53] Manzoor, M. A., Sabir, I. A., Shah, I. H., Riaz, M. W., Rehman, S., Song, C., Li, G., Malik, M. S., Ashraf, G. A., Haider, M. S., Cao, Y., & Abdullah, M. (2023). Flavonoids: A review on biosynthesis and transportation mechanism in plants. *Functional and Integrative Genomics*, *23*(3), 212. https://doi.org/10.1007/s10142-023-01147-4

[54] Pham, T. L., Ha Nguyen, T. T., Nguyen, T. A., Le-Deygen, I., Hanh Le, T. M., Vu, X. M., Le, H. K., Van, C. B., Usacheva, T. R., Mai, T. T., & Tran, D. L. (2024). Antioxidant activity of an inclusion complex between rutin and b-cyclodextrin: Experimental and quantum chemical studies. *RSC Advances*, *14*(26), 18330–18342. https://doi.org/10.1039/d4ra02307b

[55] Rashid, S. N., Hayyan, A., Hayyan, M., Hashim, M. A., Elgharbawy, A. A. M., Sani, F. S., Basirun, W. J., Lee, V. S., Alias, Y., Mohammed, A. K., Mirghani, M. E. S., Zulkifli, M. Y., & Rageh, M. (2021). Ternary glycerol-based deep eutectic solvents: Physicochemical properties and enzymatic activity. *Chemical Engineering Research and Design*, *169*, 77–85. https://doi.org/10.1016/j.cherd.2021.02.032

Figure 1

Rutin content of AMLE obtained using different NADES formulations. Values represent means ± standard deviations (n = 3). Different letters indicate significant differences based on one-way ANOVA followed by Tukey's HSD at $p < 0.05$.
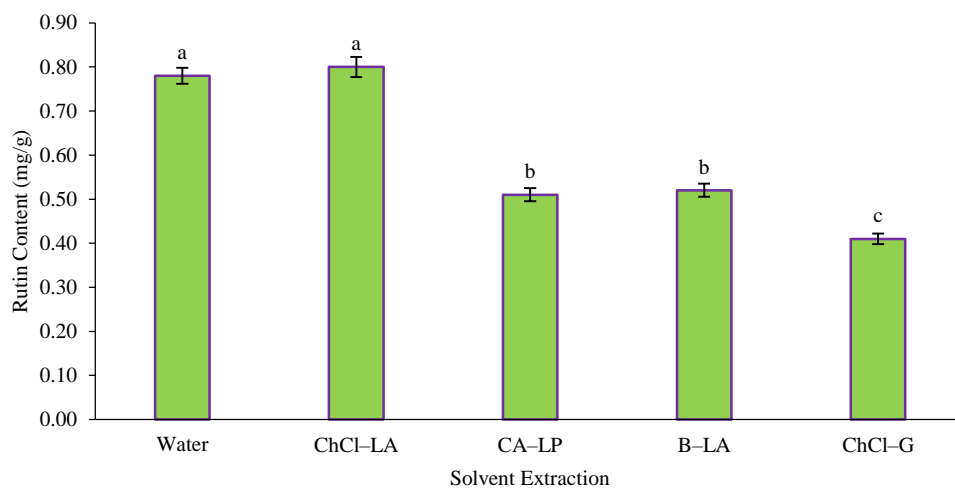
Figure 2

TPC (bar) and TFC (line) of AMLE obtained using different NADES formulations. Values represent means ± standard deviations (n = 3). Different letters indicate significant differences based on one-way ANOVA followed by Tukey's HSD at $p < 0.05$.
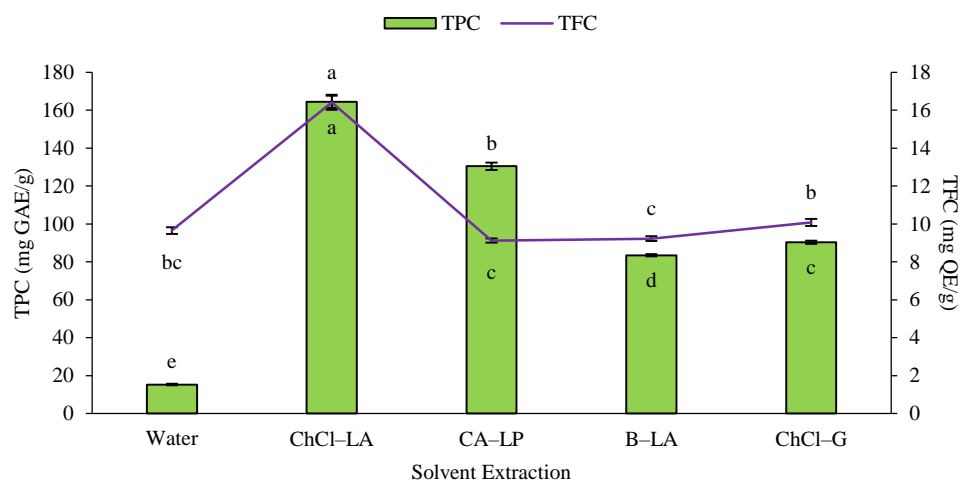
Figure 3

DPPH (bar), ABTS (bar), and FRAP (line) of AMLE obtained using different NADES formulations. Values represent means ± standard deviations (n = 3). Different letters indicate significant differences based on one-way ANOVA followed by Tukey's HSD at $p < 0.05$.
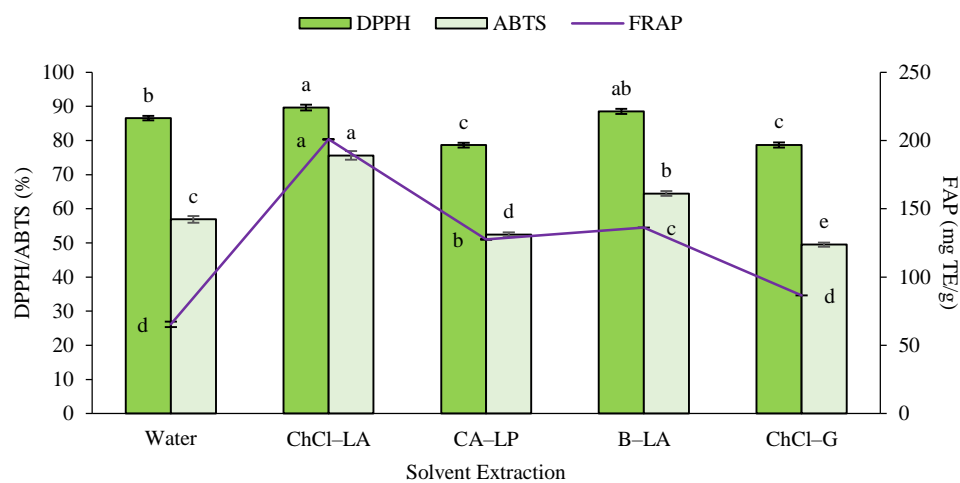
Table 1
Composition of NADES formulations used for extracting *A. muricata* leaves.

NADES	HBA	HBD	Molar ratio	References
ChCl–LA	Choline chloride	Lactic acid	1:2	[12,20]
CA–LP	Citric acid	L-Proline	1:1	[21]
B–LA	Betaine	Lactic acid	1:1	[22]
ChCl–G	Choline chloride	Glycerol	1:1	[23]

Table 2
Corrected pH and viscosity values of water and NADES systems used for AMLE extraction.

Solvent	Molar ratio	Corrected pH[*]	Viscosity (mPa·s)
Water	–	7.51 ± 0.01 [e]	0.89 ± 0.02 [a]
ChCl–LA	1:2	1.80 ± 0.02 [a]	46.00 ± 0.01 [b]
CA–LP	1:1	2.72 ± 0.01 [c]	182.00 ± 0.02 [d]
B–LA	1:1	2.52 ± 0.03 [b]	74.00 ± 0.01 [c]
ChCl–G	1:1	4.97 ± 0.05 [d]	221.00 ± 0.02 [e]

Values represent means ± standard deviations (n = 3). Different letters indicate significant differences based on one-way ANOVA followed by Tukey's HSD at $p < 0.05$. [*]Corrected pH values were obtained after applying calibration offsets derived from standard buffer solutions (pH 4, 7, and 10).

Table 3
Pearson correlation coefficients between phytochemical content (rutin, TPC, and TFC) and antioxidant activities (DPPH, ABTS, and FRAP) of AMLE.

	DPPH	ABTS	FRAP
Rutin	0.712[*]	0.663[*]	0.273
TPC	–0.026	0.450	0.889[*]
TFC	0.506	0.799[*]	0.677[*]

[*]Correlation is significant at $p < 0.01$ (two-tailed).